



Satellite, drone and video camera multi-platform monitoring of coastal erosion at an engineered pocket beach: A showcase for coastal management at Elmina Bay, Ghana (West Africa)

D.B. Angnuureng^{a,*}, K.E. Brempong^a, P.N. Jayson-Quashigah^b, O.A. Dada^c, S.G.I. Akuoko^a, J. Frimpomaa^a, P.A. Mattah^a, R. Almar^d

^a Africa Centre of Excellence in Coastal Resilience, Centre for Coastal Management, SBS, University of Cape Coast, Ghana

^b IESS, University of Ghana, Legon, Ghana

^c Department of Marine Science & Tech., Federal University of Technology, Akure, Nigeria

^d LEGOS (University of Toulouse/CNRS/IRD/CNES), Toulouse, France

ARTICLE INFO

Article history:

Received 22 January 2022

Received in revised form 12 April 2022

Accepted 7 May 2022

Available online 16 May 2022

Keywords:

Remote sensing

Coastal management

Shoreline erosion

Shoreline monitoring tools

Pocket beaches

ABSTRACT

Regular monitoring of coastal areas is a prerequisite to evade any imminent erosive disaster. However, data-driven decisions become more uncertain when a monitoring platform is unable to capture events of a certain frequency. Erosion along Ghana's coastline is endemic as in most of the Gulf of Guinea countries in West Africa. The current challenge is how to document and understand the dimensions of erosion despite limited human and logistical capacity. In the present study, shoreline change was assessed by an intensive multi-platform data collection strategy deployed for a year at Elmina Bay, Ghana through the use of drones, a shore-based camera, Sentinel satellite images and a dumpy level. The potential causes and areas of erosion at Elmina were clearly identified at a very fine scale by our sediment budget calculations. While a section of the beach in front of the Elmina Castle was adequately protected by the presence of jetties, downdrift of the larger unprotected portion of the beach was out of balance with high erosion rates. Furthermore, the results revealed that frequent, local video cameras and drones are more effective for operational monitoring of shoreline changes at all time scales. Satellite imagery is also a potential alternative tool, but its low temporal resolution, compared with video cameras, makes it unsuitable for detecting daily or event-based beach changes, and is of low accuracy for practitioners and management decisions.

© 2022 The Author(s). Published by Elsevier B.V. This is an open access article under the CC BY-NC-ND license (<http://creativecommons.org/licenses/by-nc-nd/4.0/>).

1. Introduction

As in many other regions of the world (Luijendijk et al., 2018), coastal recession in West and Central Africa can occur as a result of natural or anthropogenic factors, or both (Angnuureng et al., 2013; Mimura, 2013), and when it occurs, it may continue if not firmly addressed. Sediment loss due to drift alongshore and across the shore facilitates rapid shoreline recession (Bonou et al., 2018). It is more challenging to evaluate shoreline change behaviour when the beach is anthropised. This can be exacerbated by activities such as sand mining and the presence of sea defence structures (Ndour et al., 2018; Jayson-Quashigah et al., 2019; Alves et al., 2020) that could result in high erosion, linked to the 'knock-on effect' of the groynes (Abessolo et al., 2021). The understanding of the effect of sea defence requires pre-and post sea defence assessment (e.g. Angnuureng et al., 2013; Taveneau

et al., 2021) from intensive hydrodynamic, submerged beach bathymetry, and aerial topography measurements (Anthony et al., 2016; Angnuureng et al., 2020).

The coast of West and Central Africa has been considered largely vulnerable to natural hazards and the actions of human interventions (Ndour et al., 2018; Alves et al., 2020). Despite the implementation of various measures at different but local scales, erosion has not ceased, suggesting the need to improve management by working collaboratively at the regional level to develop regional-specific solutions. The development of a holistic plan (Alves et al., 2020) is seen as a sustainable approach to management that seeks to link users/processes together rather than focus on a single particular issue and solution. To attain this, regular monitoring, promoting observation networks, national data generalization, centralization and exchange for a better understanding of coastal dynamics and pressures are encouraged. The availability of consistent data can yield a new methodology for effective coastal management.

Among the diversity of beaches, pocket beaches are prevalent among many coastlines of the world (Daly et al., 2011; Turki

* Corresponding author.

E-mail address: donatus.angnuureng@ucc.edu.gh (D.B. Angnuureng).

et al., 2013), yet the understanding of their morphodynamics remains lagging. Pocket beaches are generally relatively short (<2 km) beaches of sand, gravel or both, locked between bedrock headlands, although artificial pocket beaches between engineering work also exist. These lateral bounding conditions commonly constrain alongshore sediment supply to pocket beaches which are, thus, generally relatively narrow beaches that may show little progradation and may flank backshore bedrock, although some pocket beaches also bound lagoons, as in the case of Elmina. This constrained sediment supply and the short and narrow nature of pocket beaches may, thus, constitute an important management problem by rendering these beaches vulnerable to sediment loss and erosion caused by human interventions such as sand mining, maladapted engineering solutions, and in the future, sea-level rise (e.g., Brunel and Sabatier, 2007).

Presently, monitoring strategies use remote sensing and in situ platforms in isolation even though they can be optimally used complementarily. One challenge is the frequency at which they can be deployed (Angnuureng et al., 2020). Table 1 illustrates some pros and cons of some of these platforms. In the last three decades, high-resolution video camera systems (VCS) have advanced the monitoring of shoreline changes (e.g., Almar et al., 2012), intertidal bathymetry (e.g., Aarninkhof et al., 2003; Angnuureng et al., 2020) and measurement of wave properties (e.g., Yaniv et al., 2011; Angnuureng et al., 2016). Video-based remote sensing is particularly well-suited for cross-shore shoreline monitoring because it is fixed in one place and covers timescales from seconds to years, albeit at short spatial scales (Almar et al., 2012). Its application can be found in the aspects of assessing natural beach behaviour (e.g. Davidson et al., 2007; Smit et al., 2007), artificial nourishment efficiency (e.g. Kroon et al., 2007), and beaches dedicated to recreational use and safety (e.g. Jiménez et al., 2007). In addition to video-based remote sensing, Unmanned Aerial Vehicles (UAVs or drones) can be used to acquire good data to determine high-resolution sediment loss (Appeaning Addo et al., 2018a; Jayson-Quashigah et al., 2019), particularly in areas where a video camera cannot be set up. The spatial coverage of UAV and video systems suffices for the monitoring of bay or micro beaches. These remote techniques have aided the acquisition of morphological information to expand research works at sites where access to data has been challenging. A summary of some of these coastal monitoring approaches is indicated in Table 1. VCS and UAV are well suited for micro spatial spot checks over desired timescales. Satellite images on the other hand could be used for regional measurement of coastal changes at monthly to yearly timescales. In addition, satellite image data has been in existence for over half a century, hence providing data on most beaches that could be used as preliminary information for new measurements, particularly in less documented areas. Previously, satellite images data was challenged by poor resolution (>20–30 m) but that has changed in recent times (with metric to sub-metric resolution, such as the Pleiades (Taveneau et al., 2021), making it competitive and complementary to other methods.

Therefore, in this paper, the main goal is to test the feasibility of using multiple sources of remote sensing platforms to assess the dynamics of Elmina Bay beach, Ghana (Fig. 1) as a showcase for local management.

2. Materials and methods

2.1. Study site

In contrast to the eastern section of the Ghanaian coast, which is sandier and dynamic with more open beaches (Anthony et al., 2016; Appeaning Addo et al., 2018b; Jayson-Quashigah et al.,

2019), the central section is characterized by many rocks (Boye and Fiadonu, 2020) and pocket beaches. There is little information on this section of the Ghanaian coastline even though it currently experiences various degrees of erosion.

Elmina is a town situated along the central coast of Ghana. The beach is located between latitude 5°4'41.67"N and longitude 1°22'41.67"W to the west and latitude 5°5'52.59"N and longitude 1°18'50.63"W to the east along the Gulf of Guinea. It has discontinuous beaches, fragmented into rocky and sandy segments. One of these beaches is featured by the Elmina Castle adjacent to it and a fishing port built on the inlet of the Benya lagoon as well as sea defences constructed (Table 1) on each side of the inlet (Jonah et al., 2016) of the lagoon. Waves approach the coast from a south-south-west direction (Fig. 1) and the waves reaching the shoreline are weak due to its concave shape and the influence of jetties (Jonah et al., 2016). The lagoon inlet serves as a medium for fishermen to move to land and sea. Nearly 40 castles (Osei-Tutu, 2004) and forts built between the 15th and 18th centuries by the Europeans are situated along the coastline of Ghana. The Elmina beach accommodates three of these monuments one of which is the UNESCO's world heritage sites (i.e., the Cape Coast Castle, the Elmina Castle and Fort St. Jago) but this beach is currently facing various degrees of erosion (Boateng, 2012; Dadson et al., 2016). The presence of erosion along this stretch of the coastline requires regular monitoring, especially in that the beach has received management intervention through the construction of various coastal defence systems.

The beach under the present investigation is about a 1.5 km stretch, starting from the Elmina Castle in the west to the Elmina Beach Resort in the east (Fig. 1). The grain size for the Elmina beach is in the range of 1 mm (Anim, 2012). This is principally due to the presence of rocks amidst the sand. Despite the coarse sediment, the beach is reported to be experiencing chronic erosion (Boateng, 2012). Historically, the Elmina beach has been identified as a hotspot of erosion with reported rates ranging between −1.14 and −3.4 m/year (Boateng, 2012; Jonah et al., 2016). This erosion has led to the destruction of houses and properties, which subsequently led to the construction of jetties and revetment in 2017 to protect the Castle and nearby community.

At the moment, the source of sediment supply to many parts of the beach seems to have significantly reduced, maybe due to the jetties/revetments and other human activities. Generally, jetties trap sediments up drift, in this case on the western side of the Elmina beach while depriving sediment on the downdrift side, in this case, towards the beach resort on the east. There are two main different sea defence types on the beach:

- Two jetties (Fig. 1): At the east of the Benya Lagoon is a 130-m jetty, made of boulders aligned across-shore. It is in a good state and located at the mouth of the lagoon. There is also a 170-m jetty to the west of the Benya lagoon mouth as well, made of boulders aligned across-shore. These defences are in good state and located at the mouth of the lagoon. These were constructed in the years 2007 and 2011, respectively.
- A revetment (Fig. 1): Behind the Castle, a more recent revetment defence of about 1 km was constructed in 2017 using aligned boulders alongshore. It is in good state and protects the Castle on the West side.

As jetties and revetments exist on this coast, considerable amounts of sediment can be trapped on the updrift side, which can lead to major coastline setbacks on the downdrift side.

Generally, depths in the nearshore zone decrease towards the east, with significant shallow depths in the cove, which could have been influenced by eastward-directed sediment transport, and a substantial sediment exchange likely with the Benya lagoon

Table 1
Review of data collection methods.

Item	Dumpy level	UAV	VCS	Satellite
Longshore coverage	>1 km	>1 km	<1 km	>100 km
Best temporal resolution	Daily	Daily	Minutes	Weekly
Age	>3 decades	<2 decades	<3 decades	>3 decades
Orientation to shoreline	Perpendicular	Dynamic	Oblique	Dynamic
Data coverage	Spot checking	Micro (Spot checking)	Micro (Fixed spot)	Macro (Global or large data)
Best accuracy	cm	<10 cm	≈1 m	>3 m
Data collection	>2 persons	2 persons	1 person	Remotely
Risk to user	Risky at high tides	Spinning blades	Safe	Safe
Remote use	Not possible	Secured	Not secured	Secured
Processing time	Short	Long (dense map)	Short (light image)	Long
Georeferencing of images	No applicable	Manual	Automatic	Required GPS coordinates

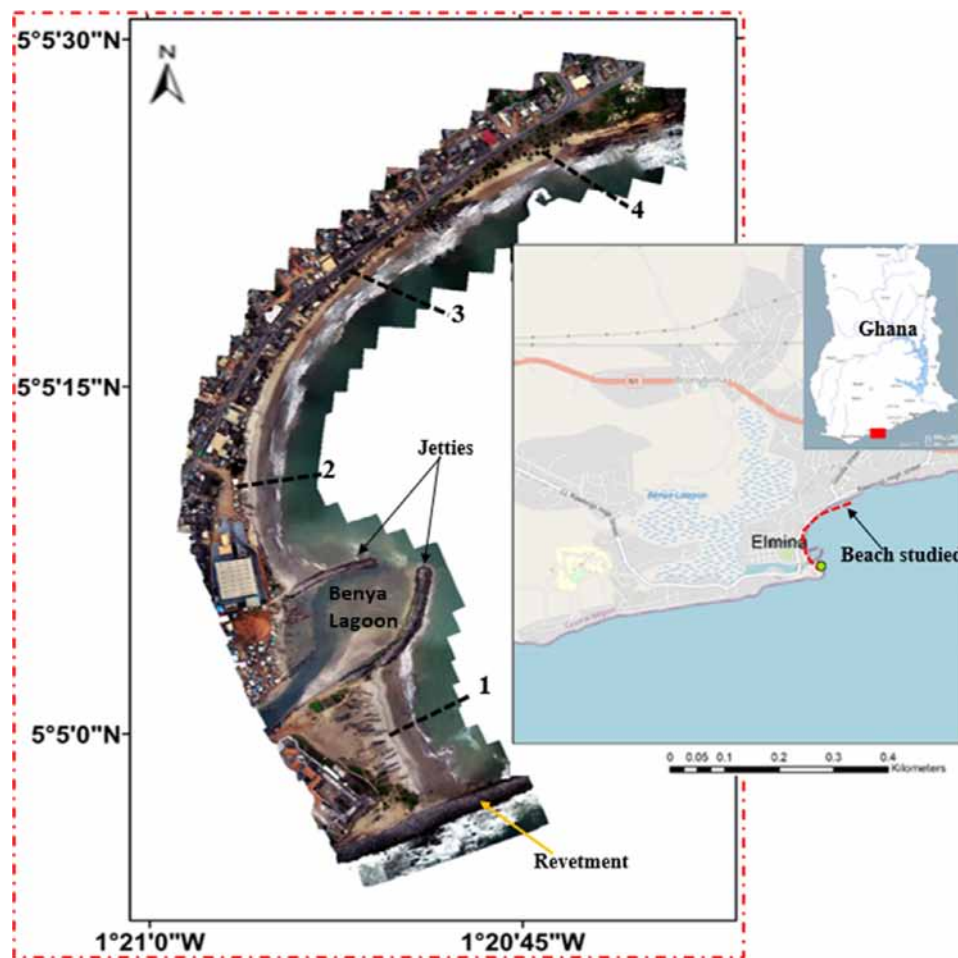


Fig. 1. (a) Map of the study site showing Elmina, inset the map of Ghana showing Elmina (a red box). (b) The orthophoto shows the four sections, Sections 1 to 4 of the Elmina beach where analysis was done. Sea defences are indicated in blue rectangles. (For interpretation of the references to colour in this figure legend, the reader is referred to the web version of this article.)

inlet. Previously, it was reported that the Benya lagoon supplies about 226 m³/year of sediment to the beach (Boateng et al., 2012). Maybe this sediment has further reduced along most parts of the beach. There are areas of high depths, specifically on the western side of the castle where sediment sink. Because of rough nearshore wave conditions, a temporal bathymetry survey is a challenging task close to the shore. Nonetheless, nearshore bathymetry has been measured to an offshore distance of about 1 km away from the castle on a total area of about 2.5 km² during this study which revealed depths ranging between 0 and 10 m.

Human activities (Boateng, 2012) such as sand mining, inappropriate management interventions (Ndour et al., 2018; Alves et al., 2020; Angnuureng et al., 2020) and global climate changes (Mimura, 2013) have been identified as major factors responsible

for coastal environment challenges in Elmina. For instance, sand mining is widespread across the Elmina-Cape Coast-Moree coastline (Jonah et al., 2016) and takes place in several forms, with the magnitude of sand taken from the beach being dependent on the transportation medium and the purpose for which sand is to be deposited. This seems to take significant toll on the beach stability with a great challenge to address along various sections of the coastline.

Despite the expected threat to life and properties, available data on nearshore physical processes, bathymetry, and human interventions that could support critical analysis and management of coastal erosion are fragmented, and incomplete.



Fig. 2. Beach profile measurements in front of the Elmina Castle using a dumpy level.

3. Materials and methods

3.1. Beach profile measurements

On August 14, 2019, we carried out beach profile measurements using a dumpy level and handheld GPS (Fig. 2). Five beach transects/profiles at about 40 m apart were measured on a 200 m wide coastline in front of the castle (Fig. 2). The profiles start from the backshore to the foreshore and were demarcated perpendicular to the beach and the baseline based on the slope. They were also used to measure the horizontal distance between slope breaks (in meters) and the values were used to determine the slope of the beach. A base station of 1.5 m high was established to serve as a point of reference elevation datum with respect to the mean sea level for the study. Relative heights were read every 5 m seaward along the transects so that many data points could be collected in less intensive time.

3.2. Multi-platform remote sensing beach monitoring techniques

3.2.1. UAV (drone)

Monthly beach surveys were carried out on this beach using DJI Phantom 4 Pro drone flights from January to December 2019. However, there was no flight in September 2019 due to some technical constraints. Ten permanent ground control points were established along the beach and coordinated to the national grid with a D-GPS. To avoid the influence of tides, drone flights were, as much as possible, conducted at low tide levels. The ground control points (GCPs) were used in geo-referencing the drone imagery. Averagely, 300 images were captured each month during each flight with a total of 11 flights in 2019. These images were manually filtered to remove blurred or overexposed shots.

A 3D scene reconstruction was performed using structure from motion (SfM) and Multi-View Stereo (MVS) algorithms (Snavely, 2011) implemented in Agisoft Metashape software. Analysis of SfM, involves (1) image alignment (Mancini et al., 2013), (2) pixel-based dense stereo reconstruction using the aligned data and the GCPs and (3) building of orthophoto and digital elevation

map (DEM). Where artificial objects such as fishing boats, coastal defences and buildings exist along the beach, the DEM was classified, as much as possible, to extract only the bare ground; thereby reducing exaggeration of topographic heights.

The 1.5 km beach was divided into four sections at random distances in relation to the presence of defences, sand and rock outcrops. Beach profiles were extracted for each section from the drone DEM for each of the months in an ArcGIS platform. The beach profiles were extracted from the lower foreshore to the berm crest. Total errors estimated on the vertical elevations (Z) and horizontal locations (XY) were 0.6 and 7.0 cm, respectively.

Orthophotos generated from the UAV images were uploaded into ArcMap. Shorelines were manually digitized using the high water mark (HWM) as a proxy (Boak and Turner, 2005) from each of the orthophotos, in order to be consistent with the proxies used for shoreline studies in Ghana (Jayson-Quashigah et al., 2013; Wiafe et al., 2013; Angnuureng et al., 2020). Orthogonal transects were cast at 5 m intervals to cross the shoreline positions, and these were used to compute the rates of change.

Shoreline rates of change and horizontal shoreline mobility were computed statistically following the Linear Regression Rates (LRR) method of the Digital Shoreline Analysis System (DSAS; Thieler et al., 2009). LRR allows the computation of the rates of change using all shoreline data and it was adopted for the rates of change estimation along the entire coastline under study.

3.2.2. Video camera system (VCS)

A video camera system (VCS) with a 180° field view was mounted on the about 40-m-high edge of the Elmina Castle wall in November 2018. The VCS was installed about 80 m from the shoreline. The final processed beach area on each video image was approximately 250 m wide in front of the castle. Timex images, defined as the average of a 15-min set of snapshots (Holland et al., 1997; Angnuureng et al., 2020), were selected and the shoreline positions were automatically extracted following the minimum shoreline variability method (Almar et al., 2012). Almar et al. (2012) have shown that beach sand displays high red colouration (R) and low green (G) pigments, thus yielding

a high ratio of R to G onshore and low R to G in water. From their work, based on some bimodal distribution, the local minimum of this distribution curve represents the transition between water and beach, that is, the shoreline position. The shoreline is represented by the time-averaged waterline where the ratio was unity. To improve accuracy, where the ratio is below 0.98 or greater than 1.1, no shoreline was extracted. These pixel data were converted to metric values by geo-referencing with ground control points collected with differential GPS. The shoreline change rates were then estimated with the median point rate (MPR). For the MPR method, the shoreline change rate (Δy) for all months was estimated by simply finding the difference between alongshore-averaged shoreline positions and the overall median position.

3.2.3. Satellite images

CoastSat toolkit (Vos et al., 2019), an open-source software toolkit written for Python 3.6 or higher, can be used to obtain time-series of shoreline positions at any sandy coastline worldwide from publicly available satellite images imagery. It employs the functionality of several freely available Python software packages. In the current study, Sentinel-2 satellite images were accessed from January 2019 to December 2019 from the GEE archive. Using the functionalities provided within the CoastSat toolkit;

(i) pre-processing of the multispectral images (cloud masking, pan sharpening and down-sampling); (ii) sub-pixel resolution shoreline extraction; and (iii) shoreline positional change measurements along shore-normal transects were conducted.

The Google Earth Engine (GEE) Python API package was used to access the satellite images imagery of Elmina, while machine learning and image processing packages, namely scikit-learn (Pedregosa et al., 2011; Vos et al., 2019) and scikit-image (van der Walt et al., 2014; Vos et al., 2019), were employed to automatically extract the position of the shoreline from the multispectral imagery. Four transects, as shown in Fig. 1, were drawn across-shore and the shoreline positions were extracted at each transect for all the months of all available sentinel images. The MPR approach is inbuilt within the CoastSat toolkit. To estimate the shoreline changes, the MPR approach was applied to remove median positions from the alongshore-averaged shoreline positions of all transects for all months. The shoreline changes were then analysed for the four sections to represent the temporal changes.

3.3. Waves and tide

ERA-5 Reanalysis (C3S, 2017) wave data was used to assess the wave climate of the area and its potential influence on coastal dynamics. ERA5 is the 5th generation ECMWF reanalysis for the global climate and weather for the past 4 to 7 decades (C3S, 2017). These wave data are produced and archived on a different grid to that of the atmospheric model, namely a reduced latitude and longitude grid. The horizontal resolution of the wave data of ERA5 is about 52 km (C3S, 2017; Bruno et al., 2020).

This data is at nine grid locations of the entire coastline of Ghana. The grid size is coarse in spatial coverage and does not fall within the length of Elmina beach, which means the ERA5 data is only used here as a representative of regional wave forcing. The closest grid swath is around Komenda, between 1.15–1.50°W and 5.03–5.13°N, which is about 20 km from Elmina. Significant wave heights of combined wind waves and swells (H_s), peak wave periods (T_p) and wave direction ($wdir$) were downloaded at six-hourly intervals. Wave condition variations were assessed in line with the time of image acquisition and shoreline changes.

There is no measured water level data for Elmina. Water levels were extracted from the WXTide model (Flater, 2010) at 15-minute intervals. This is a free Windows tide prediction program.

The tide data was used to correct the shoreline variations which were extracted from Sentinel-2 satellite images, UAV flights and VCS.

As shown in Fig. 3 a–c, the computed monthly mean significant wave height, H_s (Fig. 3b) increased gradually from about 0.8 m in January (dry season) to a peak of about 1.2 m in July (wet season), and eventually decreased to 0.84 m in December (dry season). Generally, the mean wave periods, T_p (Fig. 3a) varied between >10 s and <12 s with the peak in May and July (wet season). The $wdir$ (Fig. 3c) are generally southwesterly and ranged between 180° and 186°, with the highest $wdir$ value (more SW) observed in September 2019 and the lowest (more southerly) in April 2019. Fig. 3d presents the astronomical tides that were extracted. The beach is a microtidal zone with average heights of 1 m at daily intervals.

4. Results

4.1. Description of the seasonal beach profile evolution

The cross-shore beach profiles that were measured with the UAV are presented in Fig. 4. The slopes of the beach were estimated as the ratio of the average profile elevation to the seaward distance. The sectional variations of the beach presented a dominant reflective beach with quite steep slopes that averagely ranged from 0.04 to 0.13. The beach width decreases from sectors 1, 3, 4, to 2 (Fig. 4). The most accreted profiles varied from sector to sector probably because this is a bay beach, with a diverse direction of wave conditions incidence. For all the monthly profiles (Fig. 4) that were extracted from the UAV flights, sectors 1 and 3 profiles present highly dynamic accretion–erosion patterns. These profiles seem to suggest averaged accreting and eroding beaches, respectively.

In Section 1, the survey of the beach profile using dumpy levels revealed gentler or dissipative beaches with an average annual slope of 0.04. The vertical range of the profile envelope data shows that the topography of Section 1, on about 200 m longshore beach length, has changed by approximately 1 m in elevation on the foreshore while the backshore remains unchanged within the year. This elevation is however subject to uncertainties due to the presence of several parked fishing boats as well as sea defence structures on the beach, which results in topography undulations. In December 2019, accretion occurred on the foreshore and the beach widened to about 80 m (Fig. 4a). Overall, the January profile was the most eroded. During the field surveys, most of the beach users were found on this side of the beach, mostly for recreation.

Section 2 (Fig. 4b) is shorter in width, steeper and longer in longshore length, and about 50% larger and dominantly sandier than the rest of the Sections. The profile variation in this section (Fig. 4b) was small and uniform compared to adjacent profiles and the beach was steeper and more reflective. The mean slope of profiles in Section 2 was estimated to be 0.13.

Profiles in Section 3 were wider and more variable than those in Sections 2 and 4. Section 3 varied across the entire profile. Sections 2 and 3 were both sandy and open to the waves. Fig. 4 suggests that in Sections 2 and 3, the December profiles rather were more eroded in contrast to Section 1. The average slope of Section 3 is 0.08. The beach fronting Section 3 has a large variation between months, especially at the foreshore.

Sections 2 to 4 are more open to the sea unlike Section 1 which was in between jetties. However, Section 4 is backed by rocks, and as shown in Fig. 4d, the profile presents several bar-like features. These are rocky outcrops at the Section. At the time the data was collected for this study, the beaches in Sections 2 to 4 were unprotected and open to larger wave attacks compared to Section 1 but are now protected with rocky sea walls.

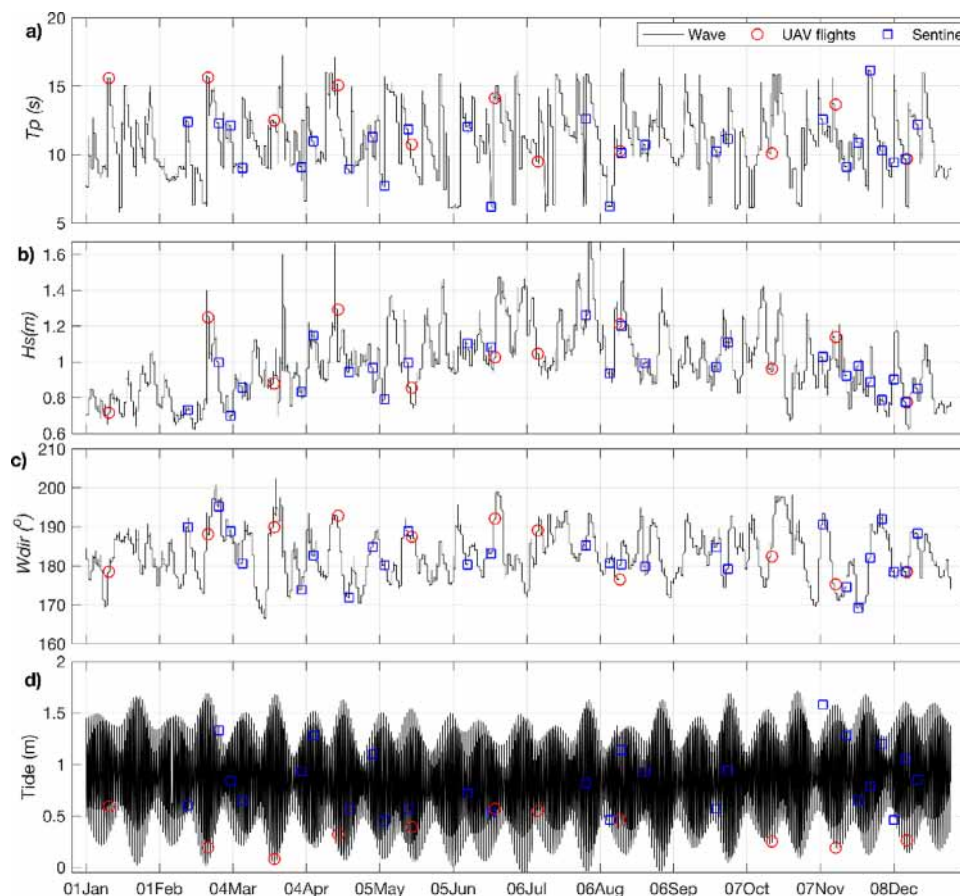


Fig. 3. Hydrodynamic forcing at Elmina Bay. (a) Peak periods of the wave, T_p (b) significant wave heights, H_s (c) wave direction, $wdir$ of ERA 5 reanalysis at Elmina, (d) tide range, TR ; Red circles indicate time of drone flights and blue squares indicate the time of Sentinel imagery.

4.2. Capturing seasonal shoreline position from multiple remote sensing sources

As shown in Fig. 5a, the alongshore-averaged ($\langle X \rangle$) shoreline positional changes for the platforms used were computed with data for all months as earlier explained. VCS shoreline positions ranged between 25 m and 43 m, excluding a distance of 80 m from the camera location. UAV shorelines were digitized in ArcMap with a baseline created at about 20 m from the first shoreline. Thus, the UAV $\langle X \rangle$ varied between 20 m and 40 m. Sentinel data obtained with the CoastSat toolkit varied between 20 and 50 m. Shoreline change rates were computed by subtracting the shoreline position of the oldest shoreline from the median of the youngest shoreline. Monthly shoreline changes that were estimated showed erosion of -8 m and accretion of about 17 m.

As shown in Fig. 5a, the shoreline highly advanced during October, November and December 2019 while retreat began in February and peaked in April. The average rates of shoreline changes were found to be 1.7, 2.8, and 1.0 m for Sentinel, UAV and VCS platforms, respectively, over the entire period. Considering individual platforms, changes from the Sentinel satellite images data had a wider range of variations (Fig. 5a). The monthly cross-shoreline changes observed from the UAV were mostly consistent with those changes observed from the Sentinel, particularly from October to December. Despite the sectoral variations in erosion and accretion by transects after a year of observations, the entire beach followed an accreting trend though most months recorded sediment loss. The monthly cumulative rate of change was approximately 2 m of accretion in 2019. This result is a consequence

of activities such as the presence of the defences at some portions (Angnuureng et al., 2013) and the fluctuations of sediment between the lagoon estuary and the sea.

The influence of tide on the cross-shore shoreline positions was computed for all three methods (Fig. 5b). The various approaches reacted differently to tides particularly when data collection coincided with spring tides. From our data, the shoreline positions from sentinel varied between 20 and 50 m but the accuracy of sentinel shoreline positions was very poor. The accuracy ranged between 0 and 15 m due to spatial resolution, tides and image processing. Shoreline positions from UAV and VCS on the other hand, with the same range of tide values, were less affected, with much higher accuracy or lesser error. The accuracies were estimated by a ratio of the tide to beach slope at the time of image collection. The averaged uncertainties due to tides were respectively, 6.7, 3.0 and 3.5 m for sentinel, VCS and UAV on horizontal shoreline position. The difference in the values of accuracies highlights the importance of the various approaches.

The seasonal shoreline positions extracted from the sentinel-2 satellite images, Timex images of the fixed VCS and monthly UAV flights at Section 1 are presented in Fig. 5c–e. The shoreline evolution showed seasonal change patterns. The seasonality as observed from the Sentinel satellite images, VCS and UAV indicate that the largest variations occurred during the Harmattan season (November to March). These periods were characterized by both increasing and decreasing hydrodynamic conditions experienced in the study area (Fig. 3), which could result in 3D features and non-uniform beaches. The Elmina shoreline position showed larger variations from the satellite images and low variation in the VCS and UAV data within the year (Fig. 5c–e). We observed

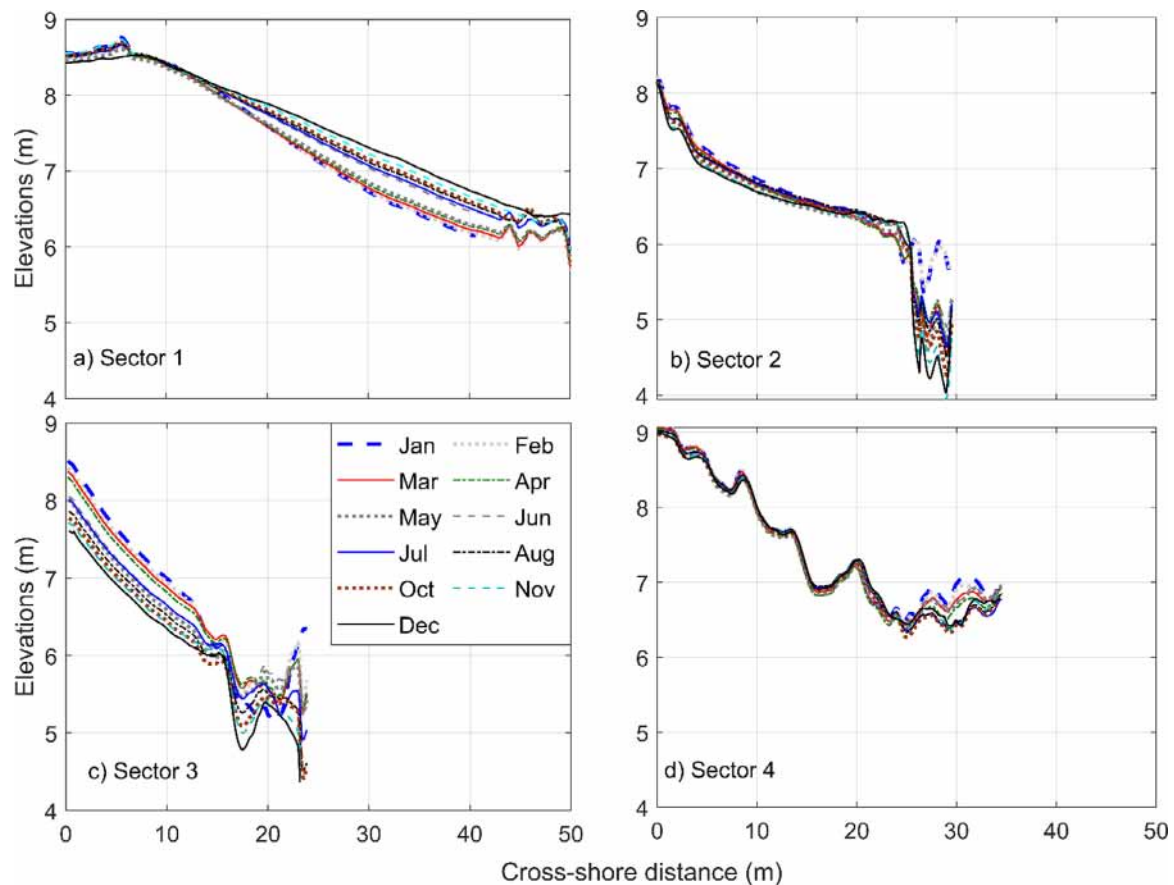


Fig. 4. a–d. Monthly UAV topographic profiles variations between January and December 2019 for Sections 1, 2, 3 and 4, respectively (see Fig. 1) on the beach.

that the shoreline positions moved more seaward from October to December (Dry season) and more landward between March to August (Wet/ Rainy season). On the other hand, the data shows that the Rainy season which is characterized by moderate to high energy conditions present less variable shoreline patterns, probably due to dissipative beach conditions.

5. Discussion

5.1. Beach change and the potential drivers

The overall beach changes presented were computed using all shorelines in the alongshore and cross-shore directions using the linear regression rate (LRR) method (Thieler et al., 2009), as shown in Fig. 6a. Along the entire study area, the maximum beach accretion was about 15 m, particularly close to the jetties while the highest erosion during the period of study was 3 m. Specifically, LRR results revealed that the observed erosion was highest between transects 500-m and 700-m as one moves down-drift away from the castle (Fig. 6a). This result is consistent with erosion rates of 3.4 m/year observed by Boateng (2012) in the same area.

In all, 20% of the entire study area experienced erosion at rates of about 3 m. As shown in Fig. 6a, large portions of Sections 3 and 4 are in disequilibrium and will probably be eroded. In Fig. 6b, we present sediment volume changes for all months at the various sections. The volume changes were usually estimated by finding the difference between sediment volumes of consecutive months.

- Section 1 is observed to be generally accreting. For Section 1, which is protected by a revetment and jetties, the beach is more stable with no record of erosion, but very high

rates of accretion (~ 3 m/year). This is revealed from the UAV profiles and VCS analyses with the beach building up from January to December, a seaward advancement of the beach for this section. Though erosion may have occurred in Section 1, the accretion is larger. The results in Fig. 6a suggest that at the frontage of the castle, the shoreline is almost at the same position and thus it may be in a stable state for a long time while the rest of the beach would likely be unstable. Based on our observation, if there will be shoreline instability in Section 1 in the future, it would be due to the topography which is low and of gentle slopes. Our findings revealed that sediment volumes accumulated throughout most parts of the year (over 54%).

- In Section 2, the results (Fig. 6a) indicate no erosion near the jetty. Shoreline changes of most individual transects show that the shoreline is advancing cumulatively seaward, which could be explained by the sediment released by the Benya lagoon that supplies about $226 \text{ m}^3/\text{year}$ of sediment to the beach (Boateng et al. 2012). However, on moving eastward away from the jetty, the beach begins to experience sediment losses. Averages over the months (Fig. 6b) show some losses of sediment in this Section. The whole period of March to July showed no recovery or accumulation of sand on the beach. The cause of these high changes observed in these months is not clear but it may be due to a combination of any of the following: cross-shore sediment transport, sand mining at the beach, the image acquisition time, intermittent storm events, wave seasonality owing to seasonal variations (Fig. 3; Dada et al., 2016) and tide-induced errors (Fig. 3d).

A moderate correlation ($r \sim 0.45$) was observed between ocean forcing (waves and tides) and beach change. This

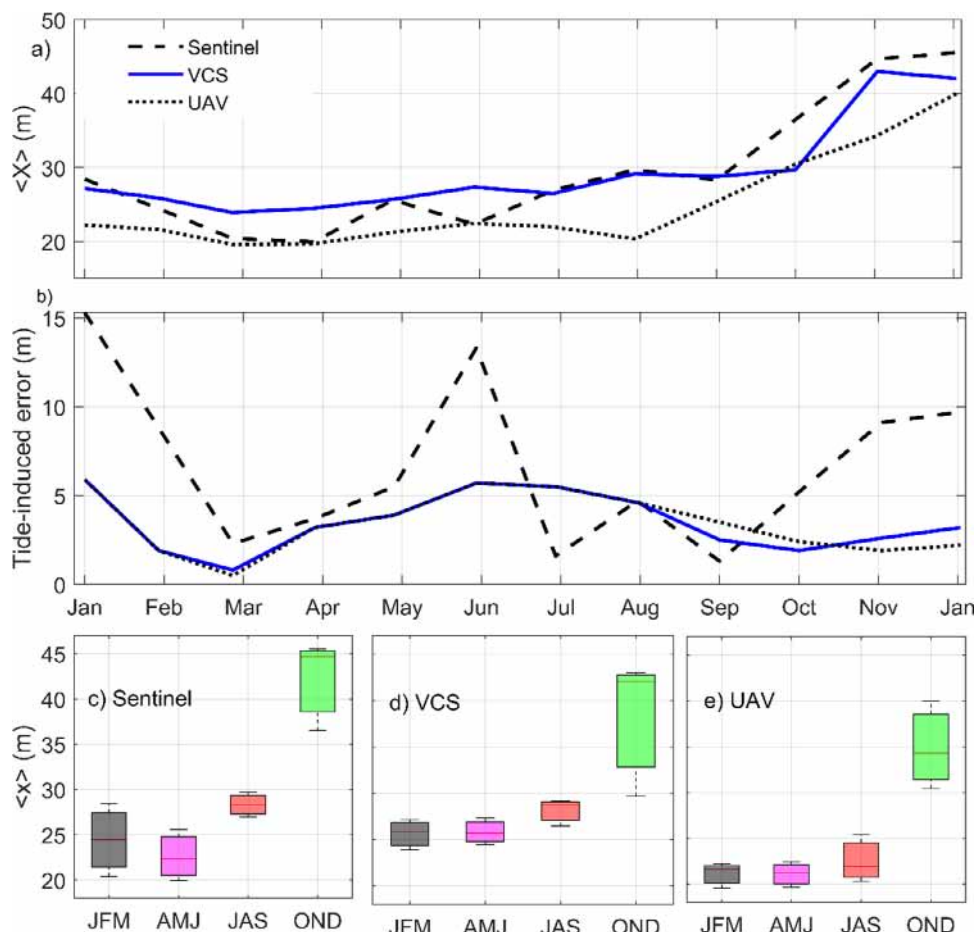


Fig. 5. Seasonal shoreline position from remote sensing platforms. (a) Monthly shoreline positions from Sentinel satellite, VCS and UAV in 2019; (b) Monthly error induced by the tide on shoreline positions; (c) Mean seasonal shoreline positions obtained from Sentinel satellite (d) Mean seasonal shoreline positions obtained from VCS; (e) Mean seasonal shoreline positions obtained from UAV; From c to e, the boxes and error bars represent the standard deviation from mean positions.

confirms that the beach change may not be solely due to waves. For instance, the area in Section 1 in front of the castle, 0–200 m (Fig. 7), between the two jetties was poorly correlated ($r \sim 0.0$; $p > 0.6$) with waves. The results suggest that wave energy is low, obviously because of the geometry of the beach as a pocket beach or the effects of the jetties. Section 2 is the sandiest part of the beach where illicit sand mining occurs by the inhabitants (Jonah, 2015). Thus, sand mining in combination with the presence of the sea defences and nonlinear wave propagation owing to irregular coastline shape could play a significant role in the beach changes. Downdrift, Sections 3 and 4, experience higher erosion up to a -3 m/year (Fig. 6a). This high rate of erosion compares well with rates observed by previous studies in the area and along the Eastern Coast of Ghana (e.g., Boateng, 2012; Jonah, 2016; Appeaning Addo et al., 2018b; Jayson-Quashigah et al., 2019). The main cause of the changes is unclear but based on our findings, it may be due to the wave conditions, the effects of the sea defence located about 400 m to the west and sand mining. These factors are heavily resident on this side of the beach. Away from the jetty sea defence, waves seem to have a high influence; the correlation between shoreline variation and waves was observed to be $r > 0.5$ with $p < 0.05$. These parts of the beach are open to wave breaking, yet there is no defence system. Thus, it was exposed to direct wave action with no management intervention at the time of the study. The erosion here has led to the destruction of previous seawalls, houses and infrastructure

along this stretch of the coast. As in Section 2, in Section 3, most months recorded sediment losses. Towards Section 4, where the beach is a bit rocky, sediment loss reduces but the shoreline retreat is high. Even though the government has a plan to protect this beach with gabion revetments, such an effort could further lead to future instability of the beach and cause erosion of large portions of the beach in the downdrift sections, from Sections 2 to 4, if not properly implemented. Overall, Fig. 6b shows that March, June and December are the months when sediment losses occurred in all Sections. We observed more sediment loss during Harmattan (November to March), and also from June to September.

Elmina beach is characterized by natural drivers and human interventions in various ways, including buildings, sand mining, fishing activities, canoes, and sea defences like the jetties. Even though we did not evaluate the precise impact of human interventions, they have implications for the study area. The VCS shows that the updrift part of the beach is mostly used to dock canoes and for recreational activities. By occupying the beach with boats, these activities have the potential to reduce the width of the beach, influence the sediment distribution, and possibly account partially for beach erosion. As shown in Fig. 7, the beach was largely used to dock canoes in May, and this could have affected the estimated width and slope. Quarterly, the beach slope changed between 0.07 and 0.13 during the year; JFM - 0.12; AMJ - 0.07; JAS - 0.13 and OND - 0.08. In terms of width, the beach was widest between October and December, and the

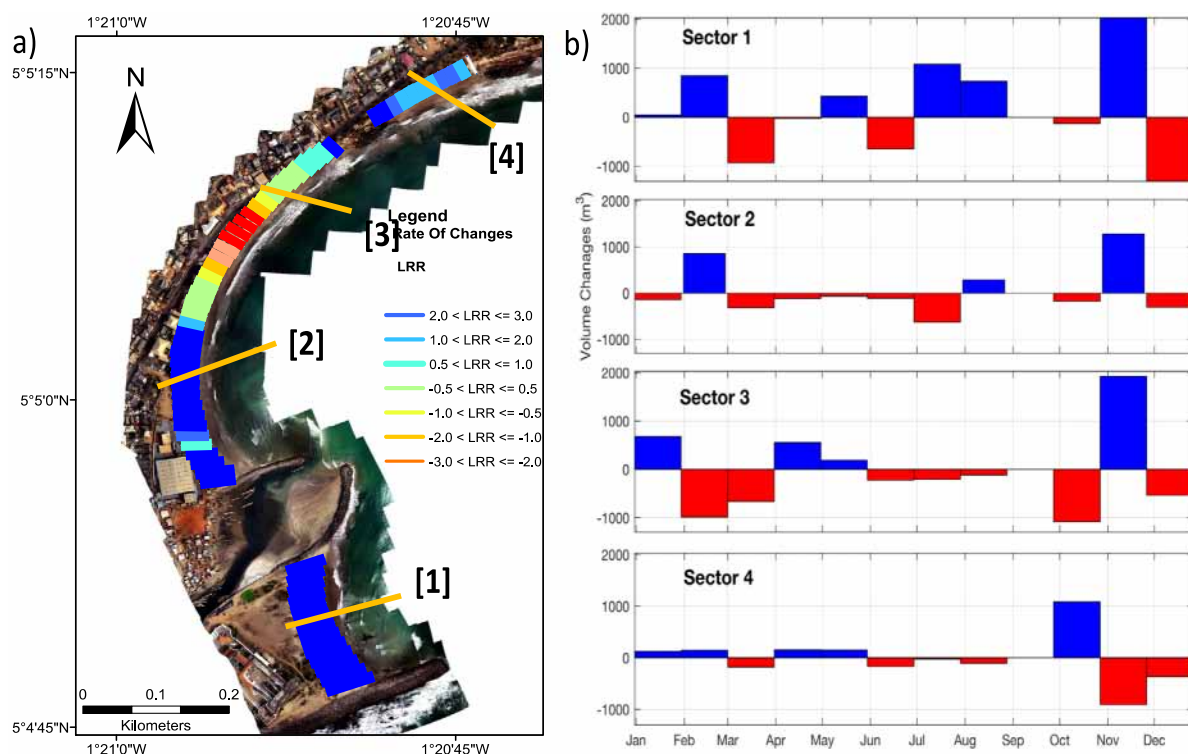


Fig. 6. (a) Shoreline change rate obtained from all monthly shorelines using LRR; Negative values means the sea is advancing landward; (b) Monthly sediment volume changes at the sectors along the beach.

narrowest between March and May. Presently, erosion occurs at some parts of the beach while others are accreting. Overall, the three platforms used here have shown the beach changes in all parts.

5.2. Performance of sentinel satellite images, UAV, and VCS platforms for monitoring beach evolution

Sentinel satellite and UAV data were provided on a weekly to monthly scale while the video camera system (VCS) was obtained daily. The performance of these platforms can be based on their ability to capture all major events that occur on the beach. As shown in Fig. 8, sentinel data, acquired on a weekly to monthly basis, is not frequent enough and cannot adequately detect intermittent – storm event – evolution, while high-frequency video-derived data can. On seasonal to interannual scales, satellite data is only able to capture about 80% of the signal at an increasing uncertainty (Fig. 8c) compared to video-derived data that shows greater significance levels. In addition, observed seasonal shoreline variations at Elmina are within the pixel resolution of Sentinel-2 (10 m) compared with UAV and VCS (0.1 m). This currently restricts the use of satellite images data for local beach management (Taveneau et al., 2021). However, a combination of large scale satellite image-derived information and the high-frequency temporal performances of the VCS has a brighter future.

5.3. Sentinel satellite images, UAV, and VCS platforms as management tools

The potential areas and causes of erosion are clearly identified at a very fine scale by our sediment budget calculations. There is a need for more careful consideration, by any hard engineering management option, particularly based on what we discussed in Section 4.2 with regards to the type of data and the accuracy that

would be obtained. These platforms have outlined the eventual sources of vulnerability of this beach as the beach profile, its slope, topography, erosion, sand mining, and the geometry of the beach. At Elmina, our results inform management about gauging the potential pitfalls associated with the emplacement of coastal housing and infrastructure. The present solutions at Elmina seem to be fighting coastal erosion, rather than managing it. The results inform management on the need for hybrid solutions such as beach nourishment to counter erosion in some areas, stopping beach sand mining and implementing hard engineering to reinforce the coastline. These methods and the potential results could be useful to the management of pocket beaches all along the central and eastern coasts of Ghana, and the approach will also be important in gauging the response of these vulnerable beaches to sea-level rise (Brunel and Sabatier, 2007).

6. Conclusions

This paper analysed the existing regular monitoring platforms as the key to the management and mitigation of potential risks with a showcase at Elmina beach, Ghana (West Africa). The potential areas and causes of erosion have been clearly identified at a very fine scale by our sediment budget calculations. When compared with a daily VCS, monthly sentinel satellite images data and UAV are effective, but insufficient to accurately detect storm events and intra-seasonal beach evolution. We have emphasized the accuracy and disadvantages of the various methods while presenting the different options to choose from for any desired study. There is a need for more careful consideration, by any hard engineering management option, of the type of data to use and the uncertainty to expect.

Our results show that due to the presence of the sea defence structures on the beach in front of the castle, no landward recession was observed at this section of the coast. The usual 'knock-on effects' from hard structures were adequately detected in the



Fig. 7. Beach occupation during the year 2019. From top to down, (a) March, (b) May, (c) September and (d) December.

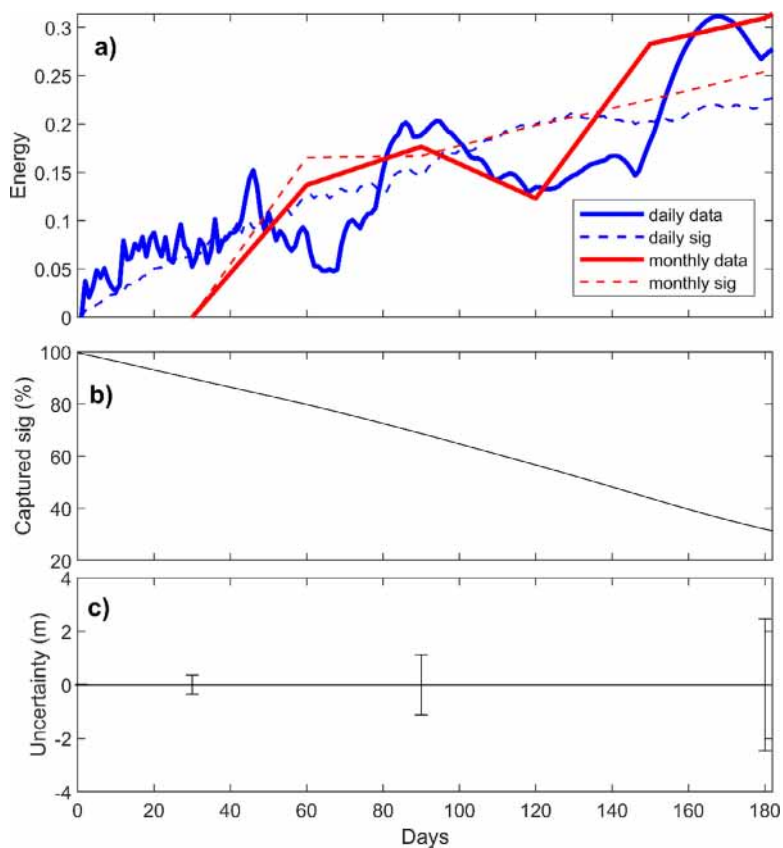


Fig. 8. The estimated performance of daily (VCS data) and monthly data (UAV and Sentinel) and the signals of VCS, UAV and Sentinel platforms.

non-protected sections which showed various degrees of erosion. Beaches situated down the drift are eroding up to -3 m over the study period. The management of the beach with only hard engineering may only be fighting the erosion, but the addition of softer solutions such as beach nourishment to counter erosion would eventually build the beach. The results of these methods could be useful to the management of other pocket beaches all along the coast of Ghana, and the approach will also be important in gauging the response of these vulnerable beaches to sea-level rise. Overall, this show-case study illustrates the potential of using multi-platform remote sensing observations to monitor coastal evolution for local coastal management.

CRediT authorship contribution statement

D.B. Angnuureng: conceptualization, Methodology, Writing – original draft, Software, Formal analysis, Funding acquisition, Project administration. **K.E. Brempong:** Investigation, Validation, Formal analysis. **P.N. Jayson-Quashigah:** Validation, Formal analysis. **O.A. Dada:** Investigation, Writing – review & editing. **S.G.I. Akuoko:** Investigation, Writing – review & editing. **J. Frimpomaa:** Investigation, Writing – review & editing. **P.A. Mattah:** Writing – review & editing, Supervision, Project administration. **R. Almar:** Writing – review & editing, Supervision, Funding acquisition.

Declaration of competing interest

The authors declare that they have no known competing financial interests or personal relationships that could have appeared to influence the work reported in this paper.

Funding

This research received funds from the National Geographic Society (CP-107T-17), USA, The World Academy of Science (17-429 RG/PHYS/AF/AC_IFR3240300132), UNESCO, Italy and the Institute of Research for Development (IRD-JEAI).

References

- Aarninkhof, S.G.J., Turner, I.L., Dronkers, T.D., Caljouw, M., Nipius, L., 2003. A video-based technique for mapping intertidal beach bathymetry. *Coast. Eng.* 49 (4), 275–289. [http://dx.doi.org/10.1016/s0378-3839\(03\)00064-4](http://dx.doi.org/10.1016/s0378-3839(03)00064-4).
- Abessolo, G.O., Hoan, L.X., Larson, M., Almar, R., 2021. Modeling the Bight of Benin (Gulf of Guinea, West Africa) coastline response to natural and anthropogenic forcing. *Reg. Stud. Mar. Sci.* (ISSN: 2352-4855) 48, 101995, 12 p.
- Almar, R., Ranasinghe, R., Catalan, P.A., Senechal, N., Bonneton, P., Roelvink, D., Bryan, K.R., Mariou, V., Parisot, J.P., 2012. Video-based detection of shorelines at complex meso-macro tidal beaches. *J. Coast. Res.* 28 (5), 1040–1048.
- Alves, B., Angnuureng, D.B., Morand, P., Almar, R., 2020. A review on coastal erosion and flooding risks and best management practices in west Africa: what has been done and should be done. *J. Coast. Conserv.* 24, 38. <http://dx.doi.org/10.1007/s11852-020-00755-7>.
- Angnuureng, D.B., Almar, R., Appeaning Addo, K., Senechal, N., Castelle, B., Laryea, S.W., Wiafe, G., 2016. Video observation of waves and shoreline change on the microtidal James Town beach in Ghana. *J. Coast. Res.* 75, 1022–1026.
- Angnuureng, B.D., Appeaning Addo, K., Wiafe, G., 2013. Impact of sea defence structures on downdrift coasts: The case of Keta in Ghana. *Acad. J. Environ. Sci.* 1, 104–121. <http://dx.doi.org/10.15413/ajes.2013.0102>.
- Angnuureng, D.B., Jayson-Quashigah, P.-N., Almar, R., Stieglitz, T.C., Anthony, E.J., Aheto, D.W., Appeaning Addo, K., 2020. Application of shore-based video and unmanned aerial vehicles (drones): complementary tools for beach studies. *Remote Sens.* 12, 394–413.
- Anim, M., 2012. Lithological Responses to Sea Erosion Along the Coastline from Gold Hill (Komenda) to Amisano (Saltpond) (MPhil Dissertation). University of Cape Coast, p. 106.
- Anthony, E., Almar, R., Aagaard, T., 2016. Recent shoreline changes in the Volta river delta, west Africa: The roles of natural processes and human impacts. *Afr. J. Aquat. Sci.* 41, 81–87.

- Appeaning Addo, K., Jayson-Quashigah, P.-N., Codjoe, S.N.A., Martey, F., 2018a. Drone as a tool for coastal flood monitoring in the Volta Delta, Ghana. *Geoenviron. Disasters* 5, 17. <http://dx.doi.org/10.1186/s40677-018-0108-2>.
- Appeaning Addo, K., Nicholls, R.J., Codjoe, S.N.A., Abu, M., 2018b. A biophysical and socioeconomic review of the Volta Delta, Ghana. *J. Coast. Res.* 34 (5), 1216–1226.
- Boak, E.H., Turner, I.L., 2005. Shoreline definition and detection: a review. *J. Coast. Res.* 214, 688–703. <http://dx.doi.org/10.2112/03-0071.1>.
- Boateng, I., 2012. An application of GIS and coastal geomorphology for large scale assessment of coastal erosion and management: a case study of Ghana. *J. Coast. Constr.* 16, 383–397.
- Boateng, I., Bray, M., Hooke, J., 2012. Estimating the fluvial sediment input to the coastal sediment budget: A case study of Ghana. *Geomorphology* 138, 100–110.
- Bonou, F., Angnuureng, D.B., Sohau, Z., Almar, R., Alory, G., Du Penhoat, Y., 2018. Shoreline and beach cusps dynamics at the low tide terraced grand Popo Beach, Bénin (West Africa): A statistical approach. *J. Coast. Res.* 81, 138–144.
- Boye, C.B., Fiadonu, E.B., 2020. Lithological effects on rocky coastline stability. *Heliyon* 6, e03539, 1–10.
- Brunel, C., Sabatier, F., 2007. Pocket beach vulnerability to sea-level rise. *J. Coast. Res.* 50, 604–609, Special Issue.
- Bruno, M.F., Molfetta, M.G., Totaro, V., Mossa, M., 2020. Performance assessment of ERA5 wave data in a Swell Dominated Region.
- Copernicus Climate Change Service (C3S), 2017. ERA5: Fifth Generation of ECMWF Atmospheric Reanalyses of the Global Climate. Copernicus Climate Change Service Climate Data Store (CDS), <https://cds.climate.copernicus.eu/cdsapp#!/home>. Accessed on 14 th August, 2020.
- Dada, O.A., Li, G.X., Qiao, L.L., Ding, D., Ma, Y.Y., Xu, J.S., 2016. Seasonal shoreline behaviours along the arcuate Niger Delta coast: Complex interaction between fluvial and marine processes. *Cont. Shelf Res.* 122, 51–67.
- Dadson, I.Y., Owusu, A.B., Adams, O., 2016. Analysis of shoreline change along Cape Coast-Sekondi Coast, Ghana. *Geo. J.* 2016, 1–9. <http://dx.doi.org/10.1155/2016/1868936>.
- Daly, C.J., Bryan, K.R., Roelvink, J.A., Klein, A.H.F., Hebbeln, D., Winter, C., 2011. Morphodynamics of embayed beaches: The effect of wave conditions. *J. Coast. Res.* 51, 1003–1007, (Proceedings of the 11th International Coastal Symposium).
- Davidson, M., Van Koningsveld, M., de Kruijff, A., Rawson, J., Holman, R., Lamberti, A., Medina, R., Kroon, A., Aarninkhof, S., 2007. The coast-view project: Developing video-derived coastal state indicators in support of coastal zone management. *Coast. Eng.* 54 (6–7), 463–475. <http://dx.doi.org/10.1016/j.coastaleng.2007.01.007>.
- Flater, D., 2010. WXTide32 - a free windows tide and current prediction program. www.wxtide32.com. Last accessed on 22/11/2020.
- Holland, K., Holman, R., Lippmann, T., Stanley, J., Plant, N., 1997. Practical use of video imagery in nearshore oceanographic field studies. *IEEE J. Ocean. Eng.* 22, 81–92.
- Jayson-Quashigah, P.N., Appeaning Addo, K., Amisigo, B., Wiafe, G., 2019. Assessment of short-term beach sediment change in the Volta Delta coast in Ghana using data from unmanned aerial vehicles (drone). *Ocean Coast. Manage.* 161, 104952. <http://dx.doi.org/10.1016/j.ocecoaman.2019.104952>.
- Jayson-Quashigah, P.N., Appeaning Addo, K., Kufogbe, S.K., 2013. Medium resolution satellite images imagery as a tool for monitoring shoreline change. Case study of the eastern coast of Ghana. *J. Coast. Res.* 65, 511–516. <http://dx.doi.org/10.2112/SI65-087.1>.
- Jiménez, J.A., Osorio, A., Marino-Tapia, I., Davidson, M., Medina, R., Kroon, A., Archetti, R., Ciavola, P., Aarninkhof, S.G.J., 2007. Beach recreation planning using video-derived coastal state indicators. *Coast. Eng.* 54 (6–7), 507–521. <http://dx.doi.org/10.1016/j.coastaleng.2007.01.012>.
- Jonah, F.E., 2015. Managing coastal erosion hotspots along the Elmina, Cape Coast and Moree area of Ghana. *J. Ocean Coast. Manage.* <http://dx.doi.org/10.1016/j.ocecoaman.2015.02.007>.
- Jonah, F.E., Boateng, I., Osman, A., Shimba, M.J., Mensah, E.A., Adu-Boahen, K., Chuku, E.O., Effah, E., 2016. Shoreline change analysis using end point rate and net shoreline movement statistics: An application to Elmina, Cape Coast and Moree section of Ghana's coast. *Reg. Stud. Mar. Sci.* 7, 19–31. <http://dx.doi.org/10.1016/j.rsma.2016.05.003>.
- Kroon, A., Davidson, M.A., Aarninkhof, S.G.J., Archetti, R., Armaroli, C., Gonzalez, M., Medri, S., Osorio, A., Aagaard, T., Holman, R.A., Spanhoff, R., 2007. Application of remote sensing video systems to coastline management problems. *Coast. Eng.* 54 (6–7), 493–505. <http://dx.doi.org/10.1016/j.coastaleng.2007.01.004>.
- Luijendijk, A., Hagenaars, G., Ranasinghe, R., et al., 2018. The state of the world's beaches. *Sci. Rep.* 8, 6641. <http://dx.doi.org/10.1038/s41598-018-24630-6>.
- Mancini, F., Dubbini, M., Gattelli, M., Stecchi, F., Fabbri, S., Gabbianelli, G., 2013. Using unmanned aerial vehicles (UAV) for high-resolution reconstruction of topography: The structure from motion approach on coastal environments. *Remote Sens.* 5, 6880–6898.
- Mimura, N., 2013. Sea-level rise caused by climate change and its implications for society. Sea-level rise caused by climate change and its implications for society. *Proc. Jpn. Acad. Ser. B* 89 (7), 281–301.

- Ndour, A., Laïbi, R., Sadio, M., Degbé, C.G.E., Diaw, A.T., Oyédé, L.M., Anthony, E.J., Dussouillez, P., Sambou, H., Dièye, E.H.B., 2018. Management strategies for coastal erosion problems in west Africa: Analysis, issues, and constraints drawn from examples from Senegal and Benin. *Ocean Coast. Manage.* 156, 92–106. <http://dx.doi.org/10.1016/j.ocecoaman.2017.09.001>.
- Osei-Tutu, B., 2004. African American reactions to the restoration of Ghana's 'slave castles'. In: *Public Archaeology*; 3/4. (ISSN: 1465-5187) pp. 195–204.
- Pedregosa, F., Varoquaux, G., Gramfort, A., Michel, V., Thirion, B., Grisel, O., Blondel, M., Prettenhofer, P., Weiss, R., Dubourg, V., Vanderplas, J., Passos, A., Cournapeau, D., Brucher, M., Perrot, M., Duchesnay, E., 2011. Scikit-learn machine learning in Python. *J. Mach. Learn. Res.* 12, 2825–2830. <http://dx.doi.org/10.1007/s13398-014-0173-7.2>.
- Smit, M.W.J., Aarninkhof, S.G.J., Wijnberg, K.M., González, M., Kingston, K.S., Southgate, H.N., Ruessink, B.G., Holman, R.A., Siegle, E., Davidson, M., Medina, R., 2007. The role of video imagery in predicting daily to monthly coastal evolution. *Coast. Eng.* 54 (6–7), 539–553. <http://dx.doi.org/10.1016/j.coastaleng.2007.01.009>.
- Snively, N., 2011. Scene reconstruction and visualization from internet photo collections: A survey. *IPSJ Trans. Comput. Vis. Appl.* 3, 44–66.
- Taveneau, A., Almar Rafaël, E.W.J., Sy, B.A., Ndour, A., Sadio, M., Garlan, T., 2021. Observing and predicting coastal erosion at the langue de barbarie sand spit around saint louis (Senegal, west Africa) through satellite-derived digital elevation model and shoreline. *Remote Sens.* 13 (13), 2454.
- Thieler, E.R., Himmelstoss, E.A., Zichichi, J.L., Ergul, A., 2009. The Digital Shoreline Analysis System (DSAS) Version 4.0 - an ArcGIS Extension for Calculating Shoreline Change. Open-File Report. US Geological Survey Report No. 2008-1278, <http://woodshole.er.usgs.gov/projectpages/dsas/version4/>.
- Turki, I., Medina, R., Gonzalez, M., Coco, G., 2013. Natural variability of shoreline position: Observations at three pocket beaches. *Mar. Geol.* 338, 76–89. <http://dx.doi.org/10.1016/j.margeo.2012.10.007>.
- van der Walt, S., Schonberger, J.L., Nunez-Iglesias, J., Boulogne, F., Warner, J.D., Yager, N., Goullart, E., Yu, T., 2014. Scikit-image: image processing in python. *PeerJ* 2, e453. <http://dx.doi.org/10.7717/peerj.453>.
- Vos, K., Splinter, K.D., Harley, M.D., Simmons, J.A., Turner, I.L., 2019. CoastSat: A google earth engine-enabled python toolkit to extract shorelines from publicly available satellite imagery. *Environ. Model. Softw.* 122, 104528. <http://dx.doi.org/10.1016/j.envsoft.2019.104528>.
- Wiafe, G., Boateng, I., Appeaning Addo, K., Quashigah, P.N., Ababio, S.D., Laryea, S.W., 2013. *Handbook of Coastal Processes and Management in Ghana*. Gloucester, UK, The Choir Press, p. 274.
- Yaniv, G., Browne, M., Lane, C., 2011. Automatic estimation of nearshore wave height from video timestacks. In: *International Conference on Digital Image Computing: Techniques and Applications*. <http://dx.doi.org/10.1109/DICTA.2011.68>.